Available online www.jocpr.com

Journal of Chemical and Pharmaceutical Research, 2014, 6(10):32-39

Research Article

ISSN : 0975-7384
CODEN(USA) : JCPRC5

A panoptic computational electrochemical profile of *p*-isobutylacetophenone-local descriptors complement antifungal activity

P. Vijaya and K. R. Sankaran*

Department of Chemistry, Annamalai University, Chidambaram, Tamil Nadu, India

---

ABSTRACT

The conformational analysis of p – isobutylacetophenone (IBAP) is initiated by potential energy surface scan of p – isobutylacetophenone using DFT method. The theoretical IR frequencies and chemical shifts are compared with the experimental results. The IR frequencies of IBAP are analysed by Potential energy Distribution calculation using Vibrational Energy Distribution Analysis (VEDA) program. The electrochemistry of IBAP studied is analysed theoretically. The determination of various reactivity descriptors in the context of chemical reactivity employing various population analyses reveals the electrophilicity of carbonyl carbon in IBAP and antifungal activity of IBAP.

Keywords: p-isobutyl acetophenone, DFT, VEDA, fukui functions, antifungal

---

INTRODUCTION

p – isobutylacetophenone (IBAP) has the pharmaceutical importance in synthesizing Ibuprofen, a non - steroidal anti inflammatory (NSAID) drug that functions by reducing the hormones which cause inflammation and pain in our body. Ibuprofen is the active ingredient in a number of pain relievers e.g., Advil, Motrin, Nuprin. Normally, hydrogenation of IBAP yields ibuprofen. Numbers of works have been reported on the absorption of IBAP, kinetics of hydrogenation of IBAP, production of ibuprofen from IBAP using different catalysts. A detailed DFT study of IBAP will complement the experimental results obtained from earlier studies. The study of the local atomic descriptors like fukui functions, electrophilicity indices will help to design various chemical reactions that would decrease the destructive effect of IBAP and increase its pharmaceutical utility. B3LYP density functional model shows reasonable good performance on the geometries of the organic compounds [1].

EXPERIMENTAL SECTION

Computational techniques:
All computational studies are carried out at Density Functional theory (DFT) level on a personal computer using Gaussian 03W program package [1]. DFT calculations are less time consuming and include a significant part of the electron correlation leading to good accuracy. The calculations are carried out with the Becke's three – parameter exchange functional with the LYP correction (B3LYP) and the basis set 6-31G (d, p) are used in appropriate calculations. The computational work has begun with the conformational analysis of the compound.

The PES of IBAP is carried out at B3LYP / 6 – 311++G (d,p)level [2]. The stable conformer is then subjected to IR frequency analysis using the same level of computation. The IR frequencies obtained at B3LYP / 6 – 311++G (d,p) level are compared with the experimental results. In addition, theoretical IR vibrational frequencies of IBAP are interpreted by means of Potential energy Distribution (PED %) calculation using Vibrational Energy Distribution Analysis (VEDA) program[3]. The normal modes assignment of the theoretical IR frequencies is visualized and substantiated with help of the GaussView 5.0 visualization program.

The GIAO ^{1}H NMR and ^{13}C NMR chemical shift calculations of the stable conformer is made in $CDCl_3$ [scrf= (solvent=chloroform)] by using B3LYP / 6 – 311++G (*d, p*) basis set. As the diffusion functions are used during the calculation the isotropic values in the calculations are subtracted from a scaling factor of 182.4656 and 31.882 to obtain the chemical shifts for ^{13}C and ^{1}H NMR respectively. The chemical shifts obtained at B3LYP / 6 – 311++G(d,p) level of computation are compared with the experimental results.

The determination of various global and local reactivity descriptors in the context of chemical reactivity is also performed and the electrophilicity at the site of carbonyl carbon in IBAP is revealed. The local reactivity descriptors like fukui functions and dual descriptor are calculated employing Mulliken population (MCA), Natural population (NCA) and Hirshfeld population (HCA) and independent single point energy calculations have been made on N – 1, N and N + 1 electronic systems (where N = 96, total number of electrons in IBAP) with same molecular geometry (devoid of any structural changes in the N – 1, N and N + 1 electronic systems) at B3LYP / 6 – 31G+(d,p) level.

The anionic form of the IBAP molecule is optimized using diffusion function during the calculation at B3LYP / 6 – 31G+ (d,p) level. The NBO calculation of the IBAP molecule and its anionic form are performed at same level of computation and the change in the hybridisation, bond order and bond length of the vital bonds during anion formation are discussed.

RESULTS AND DISCUSSION

IR frequency analysis:

The optimized geometry of IBAP is given in Fig 1 with the numbering adopted in this study. The optimized geometry of IBAP with minimal energy is subjected to IR frequency calculation at B3LYP / 6 – 311++G (d,p) level. The compound IBAP consists of 29 atoms and hence 81 normal modes of vibrations. The molecule belongs to C1 symmetry. All the modes are IR active modes. The calculated IR frequencies at B3LYP / 6 – 311++G (d,p) level are scaled by a factor 0.9668. The significant experimental [4] and computed IR frequencies at both the levels are compared in Table 1. In addition, theoretical IR vibrational spectra of IBAP are interpreted by means of Potential energy Distribution (PED %) calculation using Vibrational Energy Distribution Analysis (VEDA) program. The normal modes assignment of the theoretical IR frequencies is visualized and substantiated with help of the GaussView 5.0 visualization program. The significant experimental, unscaled and scaled computed IR frequencies are given in Table 1. None of the predicted vibrational IR frequencies have any imaginary frequency implying that the optimized geometry is located at the local minimum point on the potential energy state. The calculated IR frequencies at B3LYP / 6 – 311++G (d,p) level is found to be in better agreement with the experimental IR frequencies of IBAP [4].

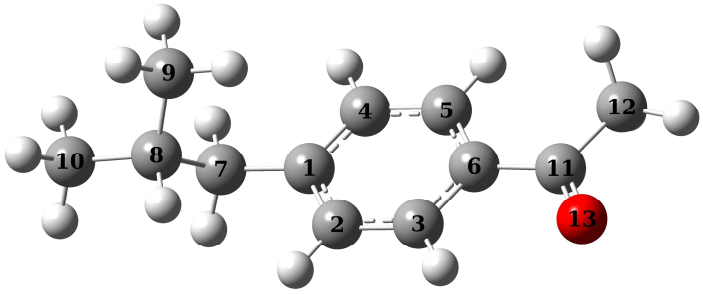

Fig 1: Optimized geometry of IBAP

^{13}C and ^{1}H NMR spectral analysis of IBAP:

NMR spectroscopy is the key to reveal the conformational analysis of organic molecule. Good quality geometries must be taken into consideration for the quantum calculation of the absolute isotropic magnetic shielding tensors to yield more reliable results. There are many reports on NMR isotropic magnetic shielding tensor calculations employing the GIAO method associated with the Density Functional theory (DFT) [5,6]. The GIAO ^{1}H NMR and ^{13}C NMR chemical shift calculations of the stable conformer is made in $CDCl_3$ [scrf= (solvent=chloroform)] by using B3LYP / 6 – 311++G (*d, p*) basis set. The experimental ^{1}H NMR [8] and ^{13}C NMR [9] chemical shift values of IBAP are compared with the computed chemical shift values in Table 2. The computed chemical shift values at B3LYP / 6 – 311++G (*d, p*) are in better agreement with the experimental chemical shift values.

Table 1: Significant experimental and computed IR wavenumbers obtained for IBAP at B3LYP/ 6– 311++G(d, p) level

Computed frequencies (cm^{-1})	Observed frequencies (cm^{-1})[4]	Vibrational assignments PED≥10% (ν – stretching vibration; β – bending vibration; τ – torsion; γ – out – of – plane bending)
3091	3085	$\nu_{C3 - H3}$(95%)
3083		$\nu_{C5 - H5}$(88%) + $\nu_{C6 - H6}$(11%)
3057		$\nu_{C6 - H6}$(88%) + $\nu_{C5 - H5}$(11%)
3054		$\nu_{C2 - H2}$(96%)
3038	3034	$\nu_{C12 - H12c}$(85%)
2992		$\nu_{C9 - H9a}$(22%) + $\nu_{C9 - H9c}$(74%)
2988		$\nu_{C12 - H12a}$(49%) + $\nu_{C12 - H12b}$(50%)
2983		$\nu_{C10 - H10a}$(61%) + $\nu_{C10 - H10b}$(35%)
2977		$\nu_{C9 - H9a}$(25%) + $\nu_{C9 - H9b}$(19%) + $\nu_{C10 - H10b}$(23%) + $\nu_{C10 - H10c}$(22%)
2971		$\nu_{C9 - H9a}$(26%) + $\nu_{C9 - H9b}$(19%) + $\nu_{C10 - H10a}$(12%) + $\nu_{C10 - H10b}$(13%) + $\nu_{C10 - H10c}$(27%)
2951	2959	$\nu_{C7 - H7a}$(45%) + $\nu_{C7 - H7b}$(49%)
2933	2924	$\nu_{C12 - H12a}$(43%) + $\nu_{C12 - H12b}$(42%) + $\nu_{C12 - H12c}$(15%)
2920		$\nu_{C7 - H7a}$(19%) + $\nu_{C7 - H7b}$(11%) +$\nu_{C9 - H9a}$(11%) + $\nu_{C9 - H9b}$(19%)+$\nu_{C12 - H12c}$(11%)
2914		$\nu_{C7 - H7a}$(18%) + $\nu_{C7 - H7b}$(17%) +$\nu_{C9 - H9a}$(14%) + $\nu_{C9 - H9b}$(34%)+$\nu_{C9 - H9c}$(10%)
2913		$\nu_{C7 - H7a}$(17%) + $\nu_{C7 - H7b}$(14%) +$\nu_{C12 - H12a}$(15%) + $\nu_{C12 - H12b}$(18%)+$\nu_{C12 - H12c}$(32%)
2902		$\nu_{C8 - H8}$(87%)
1684	1684	$\nu_{C11 - O13}$(87%)
1590		$\nu_{C2 - C3}$(33%) + $\nu_{C4 - C5}$(11%)
1550	1568	$\nu_{C1 - C4}$(27%) + $\nu_{C4 - C5}$(26%)
1485		$\beta_{H2 - C2 - C3}$(17%) + $\beta_{H3 - C3 - C2}$(17%) + $\beta_{H6 - C6 - C5}$(13%) + $\beta_{H5 - C5 - C6}$(16%) +$\beta_{C3 - C4 - C5}$(11%)
1462	1464	$\beta_{H9a - C9 - H9c}$(20%) + $\beta_{H9c - C9 - H9b}$(21%) + $\beta_{H10b - C10 - H10a}$(16%) + $\beta_{H10c - C10 - H10b}$(17%)
1423	1413	$\beta_{H12a - C12 - H12c}$(18%) + $\beta_{H12b - C12 - H12a}$(43%) + $\beta_{H12c - C12 - H12b}$(20%)
1355	1356	$\beta_{H12a - C12 - H12c}$(23%) + $\beta_{H12a - C12 - H12c}$(38%) + $\beta_{H12c - C12 - H12b}$(22%)
1271	1266	$\nu_{C10- C6}$(35%) + $\nu_{C10 - C11}$(11%)
1184	1184	$\beta_{H2 - C2 - C3}$(14%) + $\beta_{H3 - C3 - C2}$(15%) + $\beta_{H6 - C6 - C5}$(25%) + $\beta_{H5 - C5 - C6}$(15%)

Table 2: Experimental and Computational ^{1}H NMR and ^{13}C NMR chemical shifts of IBAP in $CDCl_3$ phase by DFT method Coupling constants in Hz given in parantheses

Protons	Experimental ^{1}H chemical shifts (ppm)[8]	Computed ^{1}H chemical shifts(ppm) DFT/B3LYP/ 6 – 311++G(d, p)
H(3), H(5)	7.87(d,8.4 Hz)	8.45
H(2), H(6)	7.22(d, 8.4 Hz)	7.76
H(7)	2.52(d, 7.2 Hz)	2.68
H(12)	2.56	2.64
H(8)	1.89	2.29
H(9), H(10)	0.90(d, 6.4 Hz)	0.85
Carbons	**Experimental ^{13}C Chemical Shifts (ppm)[9]**	**Computed ^{13}C Chemical Shifts (ppm) DFT/B3LYP/ 6 – 311++G(d, p)**
11	197.6	206.2
1	147.5	158.5
4	135.1	140.1
6	129.3	134.6
3	128.3	133.7
5	128.3	135.3
2	129.3	132.8
7	45.4	49.1
8	30.1	36.5
12	26.4	28.2
10	22.3	24.9
9	22.3	20.6

Electrochemistry of IBAP:

The anionic form of the molecule IBAP is optimized at B3LYP / 6 – 31G+ (*d, p*) level of computation and the selected geometrical parameters like the bond length and the torsional angles which govern the rotation of the three rotable bonds C7 – C8, C1 – C7 and C4 – C11 of the molecule in anionic form are compared with the geometrical parameters of the molecule IBAP in the neutral form. In the anionic form of the molecule the bond length of C4 – C11, C11 – O13 bonds are noticeably varied than the C4 – C11 and C11 – O13 bond lengths in the neutral molecule. The bond C11 – C12 is more elongated in anionic form of the molecule IBAP. The bond C11 – O13 is also lengthened in anionic form of the molecule IBAP. This lengthening of C11 – O13 bond in anion may be due to the conversion of C11 – O13 double bond to single bond (keto – enol tautomerism). This computational observation supports the cyclic voltammetric study of IBAP [10] in N, N – dimethyl formamide. The reduction of IBAP is found

to produce a stable radical anion. There is no much deviation observed in the torsional angles observed in both neutral and anionic forms of IBAP.

The elongation of C11 – O13 bond is well explained by the NBO analysis of the anionic form of the molecule IBAP. The NBOs of the neutral molecule and anion of IBAP are analysed. The hybridisations of the atoms involved in the formation of the vital bonds present in the isobutyl group and carbonyl group are analysed. The hybridisations underwent by the atoms involved in the formation of the vital bonds in the neutral and anionic forms of the molecule IBAP involved are presented in Table 3. Table 3 consists of the bond orders of the bonds presented. The hybridisation of the C1, C7, C8, C9 and C10 in the formation of the C1 – C7, C7 – C8, C8 – C9 and C8 – C10 appears to be unperturbed in the anionic form of molecule IBAP. Hence there is no significant change in the bond length and bond order. In the carbonyl group region of the molecule IBAP, during the formation of the anion the p – character increases with increase in the bond length and decrease in the bond order of the C11 – O13 bond. The C11 – O13 bond is found to possess a partial single bond character during the formation of anion. The π – bond in the carbonyl group of the neutral molecule formed by the overlap of p orbitals of C11 and O13 is vanished in the anionic form and that p – orbitals are supposed to be involved in the hybridisation which increases the p – character of the C11 – O13 bond in anion. The p – character decreases with the decrease in bond length and increase in bond order of the C4 – C11 bond. Hence C4 – C11 bond attains a partial double bond character during the formation of the anion. The computational NBO analysis of the neutral and anionic form of the molecule IBAP definitely complements the experimental cyclic voltammetric study of IBAP [10] in N, N – dimethyl formamide.

Table 3: Natural bond hybridisation calculated for vital bonds (NBO analysis) with bond order:

Bond	Bonded atoms	Neutral form	Bond length (Å)	Bond order	Anionic form	Bond length (Å)	Bond order
C1 – C7	C1	$sp^{2.13}$	1.513	1.00	$sp^{2.13}$	1.507	1.00
	C7	$sp^{2.65}$			$sp^{2.38}$		
C7 - C8	C7	$sp^{2.90}$	1.550	1.00	$sp^{2.76}$	1.554	1.00
	C8	$sp^{3.37}$			$sp^{2.75}$		
C8 – C9	C8	$sp^{2.69}$	1.534	1.00	$sp^{2.85}$	1.533	1.00
	C9	$sp^{2.58}$			$sp^{2.48}$		
C8 –C10	C8	$sp^{2.85}$	1.535	1.00	$sp^{2.93}$	1.535	1.00
	C10	$sp^{2.49}$			$sp^{2.39}$		
C4 –C11	C4	$sp^{2.21}$	1.497	1.02	$sp^{1.86}$ s^0p^1	1.434	1.60
	C11	$sp^{1.84}$			$sp^{1.86}$ s^0p^1		
C11 -C12	C11	$sp^{1.90}$	1.520	1.02	$sp^{2.15}$	1.536	1.02
	C12	$sp^{2.71}$			$sp^{2.45}$		
C11 –O13	C11	$sp^{2.31}$ s^0p^1	1.222	2.07	$sp^{2.33}$	1.269	1.52
	O13	$sp^{1.33}$ s^0p^1			$sp^{1.55}$		

Scheme showing reduction of IBAP

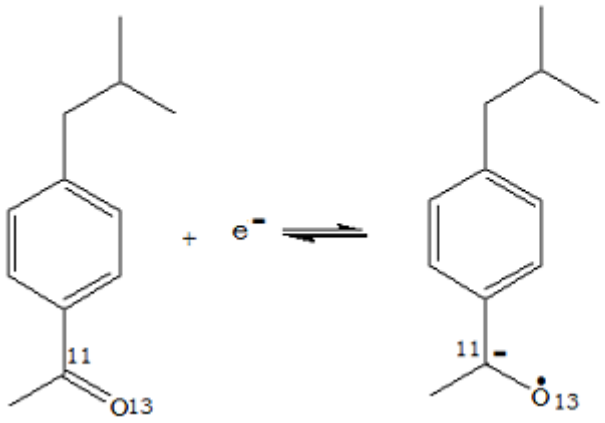

Electrophilicity index of IBAP:

According to Koopmanns'theorem[11], the HOMO energy (E_{HOMO}) is related to the ionisation potential of the molecule. $-E_{HOMO} \approx$ ionisation potential and the average value of HOMO and LUMO energies is related to the Mulliken defined electronegativity. The band gap between HOMO and LUMO is related to the hardness. The ionisation potential (I) of the molecule is determined from the difference between the energy of the N – 1 electronic system (E_{M+}) of the molecule IBAP preserving the same molecular geometry of the neutral state optimized at

B3LYP / 6 – 31G+(d,p) level and the energy of the neutral state (E_M). The electron affinity (*EA*) of the molecule is assessed from the difference between the energy of the the N + 1 electronic system(E_{M-}) of the molecule IBAP preserving the same molecular geometry of the neutral state optimized at B3LYP / 6 – 31G+(d,p) level and the energy of the neutral state (E_M).

$$I = E_{M+} - E_M \quad (1)$$
$$EA = E_M - E_{M-} \quad (2)$$

Hence, the electronegativity (χ) and the chemical hardness (η) of the molecule can be predicted as follows,

$$\chi = (I + EA)/2 \quad (3)$$
$$\eta = (I - EA)/2 \quad (4)$$

The chemical potential, μ, is the derivative of the energy with respect to the number of electrons and corresponds to the negative of the electronegativity. Hence,

$$\mu = -\chi \quad (5)$$

The electrophilicity index (ω)[12], is a measure of energy lowering due to maximal electron flow. This new global reactivity index measures the stabilization in energy when the system acquires an additional electronic charge from the environment. The electrophilicity which refers to the electrophilic power of a molecular system's ability to accept electrons is defined as

$$\omega = \mu^2 / 2\eta \quad (6)$$

The electrophilicity is a descriptor of reactivity that allows a quantitative classification of the global electrophilic nature of a molecule. The values of χ, η, μ and ω are 4.411, 4.328, -4.411 and 2.248 respectively.

The Fukui function *f(r)*[13], the widely used local density functional descriptors to model chemical reactivity and site selectivity is defined as

$$f(r) = [\partial \rho_{(\vec{r})} / \partial N]_{v(\vec{r})} \quad (7)$$

where $\rho(r)$ is the electron density at the point r, N is the number of electrons and v(r) is the external potential in which the N electrons move. The densities can be integrated over each atom and the condensed fukui function is given as

$$f_k^+ = q_k^{N+1} - q_k^N \quad (8)$$

$$f_{\bar{k}} = q_k^N - q_k^{N-1} \quad (9)$$

where q_k^N refers to the gross charge on atom k in the molecule with N electrons, q_k^{N+1} denotes the gross charge on atom k in the molecule with N + 1 electrons and q_k^{N-1} denotes the gross charge on atom k in the molecule with N – 1 electrons. f_k^+ indicates the capacity of atom k to undergo nucleophilic attack and $f_{\bar{k}}$ indicates the tendency of atom k to undergo electrophilic attack.

A dual descriptor (Δ*f*)[14] is defined as the difference between the nucleophilic and electrophilic fukui functions and is given by

$$\Delta f = f_k^+ - f_k^- \quad (10)$$

If $\Delta f > 0$, then the site is favoured for a nucleophilic attack.

The local quantity called philicity (ω_k^α) associated with atomic site *k* in a molecule with the help of the corresponding condensed fukui function (f_k^α) (where α = +, - and 0representing nucleophilic, electrophilic and radical attacks respectively) is given by

$$\omega_k^\alpha = \omega f_k^\alpha \qquad (11)$$

The condensed philicity summed over a group of relevant atoms is defined as 'group philicity' . It is obtained by adding the philicity of nearby bonded atoms.

$$\omega_g^\alpha = \sum_{k=1}^{n} \omega_k^\alpha \qquad (12)$$

where *n* = number of atoms bonded o the reactive atom.

The Mulliken charge, Natural charge and Hirshfeld charge on the atoms pictured out (Fig. 2) from the DFT analysis of the molecule IBAP and its N + 1 and N – 1 electronic forms are used to determine the f_k^+ and f_k^- values. The f_k^+ and f_k^- values are determined for the atomic sites surrounding the carbonyl carbon *viz.*, C11, O13, C12 and C4 based on mulliken charges(MCA), natural charges (NCA) and Hirshfeld charges (HCA). The dual descriptor (Δf) is calculated for atoms forming the sites for attack from the f_k^+ and f_k^- values. The q_k^N, q_k^{N+1}, q_k^{N-1}, f_k^+, f_k^- and Δf values for C11, O13, C12 and C4 atomic sites are given in Table 4. The values in Table 4 point out that the MCA and NCA scheme provide negative f_k^+ fukui function and HCA scheme provide positive f_k^+ fukui function [15]. Several research workers [16 – 19] have epitomized the usefulness of HCA scheme in the determination of the local descriptor quantities of a molecular system. The MCA scheme provides a negative Δf value for C11 atomic site which clearly predicts that MCA scheme is not able to effectively reproduce the change in the electron density around the reactive atom in these type of carbonyl compound. The NCA and HCA schemes provide a positive Δf value for C11 atomic site indicating that the carbonyl carbon C11 site is favourable for nucleophilic attack and a negative Δf value for O13 atomic site indicating that the O13 atomic site is favourable for electrophilic attack.

The group electrophilicity index value (ω_g^+) in Table 4 indicates that the value determined for the carbonyl carbon (C11) and the nearby bonded atoms (C4, C12 and O13) by MCA, NCA and HCA schemes is lesser than the group electrophilicity index value values of the earlier reported carbonyl compounds[20]. This decrease in the group electrophilicity index value and consequent decreased rate of nucleophilic attack can be attributed to the presence of electron donating alkyl group in IBAP molecule.

Pharmacological importance of IBAP:

The pharmacological importance of IBAP can be explained with the help of the determination of the electrophilicity index of the molecule at vital atomic sites. The study on the reactivity of the carbonyl carbon and oxygen reveals that the electrophilic and nucleophilic part of the molecule IBAP gets bound to the nucleophilic and electrophilic part of the biological target respectively. IBAP is subjected to *in vitro* antifungal activity test against fungal strains viz., *Aspergillus flavus, Pencillium chryogenum, Trichoderma viride, Fusarium oxysporum.* Amphotericin B is used as standard drug whose zone of inhibition are 12 to 14 mm against all the tested fungi. The activation index of IBAP (Table 6) against the tested fungi with reference to the standard antibiotic Amphotericin B is in the range of 20 – 24 which predicts that the molecule IBAP has increased antifungal activity than the standard drug Amphotericin B.

Amphotericin B binds with ergosterol [21,22], a lipid in the cell membrane of the fungi and creates a polar pore in the cell membrane of the fungi which makes the vital ions like K^+, H^+ to ooze out and kills the fungal cells. The

binding between Amphotericin B and ergosterol is between the electrophilic NH_2^+ part of Amphotericin B and the nucleophilic OH part of ergosterol. The experimental results of *in vitro* antifungal activity test of IBAP indicates that the electrophilicity index of the C11 carbonyl carbon in IBAP may be greater than that of the electrophilic power of NH_2^+ part of Amphotericin B and hence binds well with the lipid ergosterol present in the cell membrane of all the tested fungi.

Fig 2 Graph showing mulliken, natural and Hirshfeld charges derived for IBAP

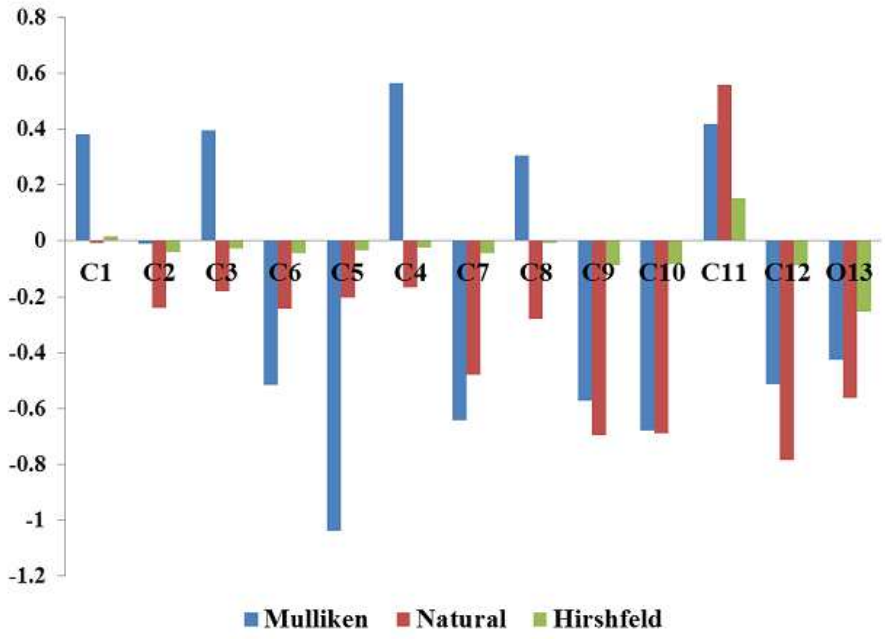

Table 10: Calculated mulliken charges, natural charges and hirshfeld charges $q_k^N, q_k^{N+1}, q_k^{N-1}$, condensed fukui functions f_k^+, f_k^-, dual descriptor (Δf), local and group electrophicity index (ω_g^+) at significant atomic sites at DFT level.

Atomic site	q_k^N	q_k^{N+1}	q_k^{N-1}	f_k^-	f_k^+	Δf	ωf_k^+	ω_g^+
Mulliken charge based analysis (MCA)								
C11	5.581	5.497	5.655	-0.073	-0.085	-0.011	-0.199	0.281
C12	6.513	6.633	6.425	0.089	0.120	0.031	0.282	
O13	8.424	8.584	8.239	0.185	0.159	-0.026	0.375	
C4	5.435	5.359	5.387	0.048	-0.075	-0.123	-0.177	
Natural charge based analysis (NCA)								
C11	5.441	5.598	5.454	-0.013	0.157	0.170	0.369	0.775
C12	6.785	6.762	6.782	0.003	-0.023	-0.026	-0.053	
O13	8.562	8.712	8.357	0.205	0.150	-0.055	0.353	
C4	6.167	6.213	6.015	0.153	0.045	-0.107	0.107	
Hirshfeld charge based analysis (HCA)								
C11	5.849	5.958	6.057	-0.208	0.109	0.317	0.256	0.748
C12	6.087	6.115	6.071	0.016	0.027	0.011	0.064	
O13	8.253	8.387	8.103	0.151	0.133	-0.017	0.314	
C4	6.024	6.072	5.940	0.084	0.048	-0.036	0.113	

Table 6: Antifungal activity of IBAP:

Name of the fungus	Zone of inhibition (mm)		Activation index(AI)*
	Standard drug Amphotericin B	IBAP	
Aspergillus flavus	14	20	1.43
Pencillium chryogenum	12	22	1.83
Trichoderma viride	13	24	1.85
Fusarium oxysporum	14	20	1.43

** AI = Zone of inhibition of sample / Zone of inhibition of standard*

CONCLUSION

The IR vibrational frequency calculation for the IBAP is carried out with the B3LYP / 6 – 311++G (d,p) basis set and the calculated values are compared with the experimental values. The B3LYP / 6 – 311++G (d,p) level of calculation is proved to be in good agreement with the experimental values. The theoretical IR frequencies were assigned to the respective vibrations with PED% using VEDA and Gauss View Visualization program. The theoretical ^{1}H and ^{13}C NMR chemical shift values calculated for IBAP at) B3LYP / 6 – 311++G (d,p) level and the chemical shift values calculated at B3LYP / 6 – 311G++(d,p) level are in good agreement with the experimental values. NBO analysis revealed the absence of intramolecular hydrogen bonding in IBAP. The NBO analysis of the anionic form of IBAP complemented the cyclic voltammetric studies on IBAP. The C11 – O13 single bond in the anion is evidenced by the increasing p character of C11-O13 hybrid orbitals and the absence of p – orbitals overlap in the C11-O13 bond. The local descriptors like the fukui functions and electrophilicity index of the molecule were calculated using the Mulliken charge, Natural charge and Hirshfeld charge. The C11 carbon atom in the molecule IBAP is found to be electrophilic and susceptible to nucleophilic attack but in a reduced rate than other reported carbonyl compounds because of the presence of electron donating alkyl groups in the IBAP molecule. The antifungal activity test of IBAP is also performed and IBAP is found to have increased activity than the standard drug due to comparatively higher electrophilicity index of IBAP than that of the standard drug.

REFERENCES

[1] N Subramanian; N Sundaraganesan; J Jayabharathi, *Spectrochimica Acta Part A.*, **2010**, 76, 259 – 269.
[2] P Vijaya; KR Sankaran, *J. Mol. Struct.*, **2013**, 1051, 180 – 187.
[3] MH Jamroz, *Spectrochim. Acta A.*, **2013**, 114, 220 – 230.
[4] SR Matkovic; GM Valle; LE Briand, *Lat. Am. appl. Res.*, **2009**, 39(2), 173 – 178.
[5] T Kupka; G Pasterna; M Jaworska; A Karali; P Dais, *Magn. Reson. Chem.*, **2009**; 38,149.
[6] JC Peralata; RH Contreras; OE Taurian; FS Oritz; DG Kowalevski; V Kowalevski, *J Mag. Reson. Chem.*, **1999**, 37, 31.
[7] N Karakaya; F Ucun; A Tokath; S Bahceli, *SDU J. Sci*., **2010**, 5(2), 220 – 229.
[8] S Chimichi; F Innocenti; G Orazalesi, J. *Pharm. Sci., 1980*, 69(5), 521.
[9] P Gogoi; D Konwar, *Org. and Biomol. Chem*., **2005**, 3473 – 3475. [www.rsc.org/suppdata/ob/b5/b509527a.pdf]
[10] J Damodar; R Ramesh Raju; S Jayarama Reddy, *Ind. J. Chem*., **2002**, 41(B), 2655 – 2658.
[11] CG Zhan; JA Nichols; DJ Dixon, *Phys. Chem.*, **2003**, 107, 4184 - 4195
[12] R Parthasarathi; V Subramanian; DR Roy & PK Chattaraj, *Bioorg. Med. Chem*., **2004**, 12, 5533 – 5543.
[13] M Elango; Parthasarathi; GK Narayanan; AMD. Sabeelullah; U Sarkar; NS Venkatasubramanian; V Subramanian; PK Chattaraj, *J. Chem. Sci.,* **2005**, 117, 61 – 65.
[14] C Morell; A Grand; AT Labbe, *J. Phys. Chem.*, **2005**, 109(1), 205 – 212.
[15] RK Roy; S Pal; K Hirao, *J. Chem. Phys.*, **2000**, 117, 1372 – 1379.
[16] R Parthasarathi; J Padmanabhan; V Subramanian; U Sarkar; B Maiti; PK Chattaraj, Internet *Electron. J. Mol. Des.*, **2003**, 2, 798 – 813.
[17] R Parthasarathi; J Padmanabhan; V Subramanian; B Maiti; PK Chattaraj, *J. Phys. Chem. A.,* **2003**, 107, 10346 – 10352.
[18] L Meneses; W Tiznado; RR Contreras; P Fuentealba, *Chem. Phys. Lett.*, **2004**, 383, 181 - 187
[19] R Parthasarathi; J Padmanabhan; V Subramanian; Maiti; PK Chattaraj, *Curr. Sci.*, **2004**, 86, 535 – 542.
[20] R Parthasarathi; J Padmanabhan; M Elango; V Subramanian; PK Chattaraj, *Chem. Phys. Lett.*, **2004**, 394, 225 – 230.
[21] JD Cleary; KM Wasan, *The antimicrobial agents Journal*., **2011**, 3, 30- 36.
[22] Y Umegawa; Y Nakagawa; K Tahara; H Tsuchikawa; N Matsumori; T Oishi; M Murata, *Biochemistry.*, **2012**, 51(1), 83 – 89.